Palm frond biochar production and characterisation

A. Md Som, Z. Wang and A. Al-Tabbaa

Geotechnical and Environmental Research Group, Department of Engineering, University of Cambridge, Trumpington Street, Cambridge CB2 1PZ, UK.
Email: am842@cam.ac.uk; zw257@cam.ac.uk; aa22@cam.ac.uk

ABSTRACT: Palm oil has been the world's main source of oil and fats since 2004, producing over 45 million tonnes in 2009. Malaysia alone has over 4·5 million hectares planted with oil palm and, based on common practice, ~300 palm fronds are pruned per hectare per year. This agricultural waste is currently either being used as roughage feed or, more frequently, being left between rows of palm trees to prevent soil erosion, or for nutrient recycling purposes. This paper proposes an alternative use for palm frond as a source of biochar. A traditional method commonly use by gardeners in Malaysia to improve soil fertility was used to produce the biochar. A shallow earth pit was dug in the ground for the carbonisation process. The process is described and the impact of carbonisation on the earth wall is analysed and presented. The process was later re-assessed by using TGA-FTIR. Most of the hemicelluloses had fully disintegrated, but the depolymerisation of the cellulose was still incomplete at the carbonisation temperature. Most of the lignin aromatic structure was still present in the biochar. The carbonisation process was repeated in the laboratory and biochar was characterised by using BET, SEM and FTIR. An adsorption isotherm study was conducted and the experimental data were fitted to the Langmuir model. The model predicted Pb^{2+} adsorption rates of 83·3 mg/g, Cu^{2+} 41·4 mg/g, Ni^{2+} 13·0 mg/g and Zn^{2+} 19·7 mg/g.

KEY WORDS: palm oil, earth pit, carbonisation

Biochar refers to the biomass-derived black carbon that is generally produced by the burning of biomass in a limited amount of oxygen that turns it into char (Lehmann *et al*. 2006). It is produced by a similar process to that used to produce general charcoal, but biochar is used solely for environmental purposes to improve soil condition, to facilitate infiltration of percolating groundwater and for carbon storage (Lehmann & Joseph 2009). These specific functions differentiate biochar from general charcoal. Biochar's complex mixtures of aromatic compounds generated during carbonisation (Lewis 1982) make it resistant to hydrolytic enzymes (Derenne & Largeau 2001). The raw materials used to produce biochar are similar to those used for activated carbon, and a variety of raw materials and production conditions have been evaluated (Yaman 2004).

The final structure and properties of biochar depend largely on its original feedstock (Wildman & Derbyshire 1991). Some of the original structure will be retained and some will turn into ash that gives rise to individual chemical properties. The traditional feedstock for biochar is woody biomass that consists mainly of cellulose, hemicelluloses and lignin. It has been shown that there is a notable difference in the physical and chemical properties of biochar prepared from a common woody material at different stage of growth (Wingate 2008). This implies that feedstock selection is very specific and should take account of the end use of the biochar.

It is a traditional practice by gardeners in Malaysia to make 'tanah bakar', or burned soil, to improve soil fertility. Generally, a shallow pit is dug and waste from the garden or household is burned in the pit. This process is repeated a few times before blackened soil or 'tanah bakar' can be scraped from the pit and used for enriching other soils, instead of using mineral fertilisers. This traditional practice is similar to those found in the Amazon that give rise to the dark fertile soil of *Terra Preta* (Steiner *et al.* 2009). Biochar has also been used as a soil conditioner. Its high pH and its cation exchange capacity are valuable in ameliorating acidic soil (Glaser *et al.* 2002). However, the direct impacts of biochar production on the soil conditions around the production site have rarely been evaluated (but see studies by Chidumayo (1994) and Ogutunde *et al.* (2004)).

In recent years, many studies have reported that biochar is able to remove heavy metals either from contaminated water or from soil. It has been used to sequester copper (Uchimiya *et al.* 2011), in the immobilisation and retention of arsenic, cadmium and zinc (Beesley & Marmiroli 2011) and in reducing the bioavailability of lead (Chen *et al.* 2006). Biochar has great potential to remediate contaminated soil. Biochar also qualifies as a low-cost adsorbent, defining low-cost adsorbents as those that originate from a by-product of other process or from waste, are abundant in nature and are produced with the lowest possible cost. The uses of low-cost adsorbent for the adsorption of heavy metals in contaminated waters have been widely reviewed (e.g., Bailey 1999; Babel & Kurniawan 2003; Gupta 2009).

This paper studies the direct impact to the surrounding earth wall of traditional biochar production in an earth pit. The production process was later repeated using TGA-FTIR and the smoke and gases produced during the charring were assessed to evaluate the environmental impact of traditional palm frond biochar production. The palm frond biochar produced in the laboratory was also assessed for its potential as an additive in soil remediation.

1. Materials and method

Our production of palm frond biochar followed the traditional practice of making 'tanah bakar', but involving the pit-burning of palm fronds instead of waste. Palm fronds were obtained from 3–3·5 year-old oil palm trees (Fig. 1). The frond was about 0·5 cm thick and trimmed into 2·5-cm widths. The

© 2012 The Royal Society of Edinburgh. doi:10.1017/S1755691012000035
https://doi.org/10.1017/S1755691012000035 Published online by Cambridge University Press



Figure 1 Palm oil trees: (a) 3–4 year oil palm oil tree; (b) Palm frond left at the bottom of the palm oil trees to dry and decompose.



Figure 2 (a) Palm fronds drying in the sun. (b) Palm frond (2·5 cm length).

fronds were further cut into two different lengths of 25 cm and 2·5 cm and left to dry in the sun to reduce moisture content, to facilitate the carbonisation process (Fig. 2).

The earth pit of approximately 1 m × 1 m × 1 m was dug manually in a silty clay soil. Figure 3 illustrates the carbonisation process. Easily combustible garden waste materials, such as dried leaves and twigs were placed at the bottom of the pit. Four bricks measuring approximately 10 cm in height were located at each corner of the pit and metal wire mesh placed on top of the mesh to cover the combustible materials. The 25-cm fronds were loaded directly onto the metal wire mesh and the 2·5-cm fronds were wrapped with several layers of aluminium foil before placing them in as well. More leaves and twigs were put on top of the palm fronds and the fire was started at the bottom of the pit. The pit was covered with tin alloy roofing sheets, and the cover was adjusted to allow air into the pit. This resulted in the 25-cm fronds being completely burned to ashes, but the aluminium-wrapped fronds were converted to biochar after four hours. Irreversible THERMAX Colotemp Crayons were used every hour to determine the approximate carbonisation temperature. Immediately after the pit was dug (prior to the burning), and again after the first carbonisation process, soil samples were collected for physical and chemical analysis based on BS 1377: Part 2 & 3: 1990.

The palm frond carbonisation process was assessed in the laboratory using Perkin Elmer STA 6000 and Perkin Elmer Spectrum 100 FTIR spectrophotometers, with an initial heating rate of 40°C/min to 150°C. The temperature was held constant at 150°C for ten minutes before it was increased at a rate of 10°C/min to 610°C. The flow rate of the N_2 carrier gas was set at 50 mL/min. The laboratory carbonisation process aimed to produce biochar for characterisation and a metal adsorption isotherm study, and was undertaken by wrapping the frond in several layers of aluminium foils and heating it at 320°C for four hours using a muffle furnace. The modified compulsive exchange method (Gillman & Sumpter 1986) was used to determine cation exchange capacity, and the pH was determined by heating 0·5 g of biochar in 50 ml water at 90°C with continuous stirring, cooling to room temperature and measuring with a 5500 EUTECH pH meter using an FET solid electrode calibrated with standard buffer solutions. Comparison on the type and amount of cation released by the biochar was conducted by immersing 1 g of each biochar in deionised water and agitating it at 150 rpm for one hour. The solution was filtered by using filter paper Whatman No 1 and tested using the Perkin Elmer 7000 Inductive Couple Plasma Optical Emission Spectrophotometer for Na^+, Mg^+, K^+ and Ca^+.

Characterisation of the palm frond and its biochar was also carried out using the FTIR spectrophotometer, followed by the scanning electron microscope JEOL 5800 SEM. Surface area determination was done by the BET (Brunauer–Emmett–Teller) nitrogen adsorption machine TriStar 3000 V6.04 A.

Metal isotherm studies were conducted by immersing 1 g of each biochar in different concentrations of $Pb(NO_3)_2$, $Cu(NO_3)_2$, $Ni(NO_3)_2$ and $ZnCl_2$ agitated at 150 rpm until equilibrium was reached. The solution was filtered by using filter paper Whatman No 1 before testing using the Perkin Elmer 7000 Inductive Couple Plasma Optical Emission Spectrophotometer.

https://doi.org/10.1017/S1755691012000035 Published online by Cambridge University Press



Figure 3 (a) Earth pit (b) Palm oil frond in the pit (c) Covering the earth pit zinc alloy once fire is lighted (d) Fully covered earth pit.



Figure 4 Impact of carbonisation on the earth pit wall: (a) before carbonisation; (b) after carbonisation.

Table 1 Chemical and physical characteristic of soil surrounding the earth pit before and after the carbonisation process.

Parameters		Before	After
pH		4·3	6·7
Organic Content	%	1·3	3·4
Moisture Content	%	65	6
Particle size distribution			
Gravels	%	–	–
Sand	%	4·8	3·5
Silt	%	38·6	40
Clay	%	56·6	56·5

2. Results

2.1. Biochar production

The carbonisation temperature in the earth pit was found to be approximately 320°C. Figure 4 shows the impact of fire on the surrounding earth pit wall.

Table 1 illustrates the basic physical and chemical characteristics of the soil before and after carbonisation. The particle size distributions of the soil remained essentially unchanged, unlike in the finding of Ketterings *et al.* (2000) in a study of the effects of 'slash and burn' on forest soil. However, this dissimilarity may have been due to heat loss into the soil, as a function of not just surface temperature but also of the duration of heating, soil water content and soil pore distribution (Steward *et al.* 1990). Some of the fine sand might also have disintegrated, increasing the silt content. Increase in organic content was as foreseen (Steiner *et al.* 2009) and there was a noticeable rise in pH. Soils under charcoal-making kilns have

https://doi.org/10.1017/S1755691012000035 Published online by Cambridge University Press

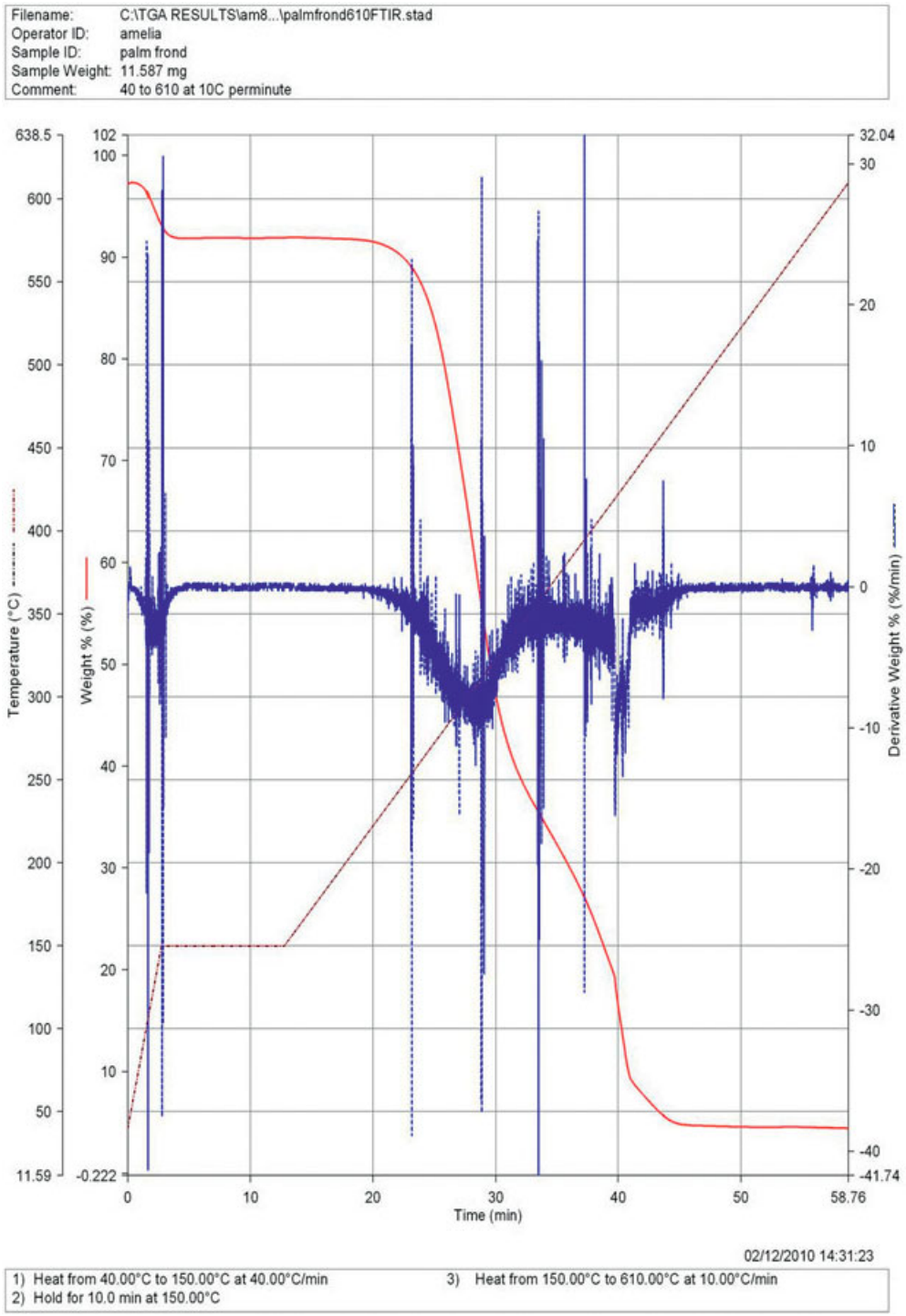


Figure 5 Thermogravimetric curve of temperature (°C), weight percent (%) and weight derivative (%/min) against time (min) during palm frond carbonisation. The weight derivative identifies the point where weight loss is most apparent.

been reported to have a pH of 7·0 compared to that of the surrounding soil of 5·5 (Chidumayo 1994) and 7·6 as compared to 5·8 (Oguntunde *et al.* 2004). However, Steiner *et al.* (2007) reported that the addition of biochar to the soil only increases the pH value by 0·12 units, and Lehmann *et al.* (2003) found that the pH value of soil in a pot experiment increased by 0·36 and 0·75 units after the addition of biochar. Tryon (1948) reported an increase in pH value from 5·15 to 6·10 only after the addition of 45% charcoal. The increases in soil organic matter and pH values may have been the reasons for the soil becoming more fertile when biochar is used to ameliorate acidic soil.

2.1.1. TGA-FTIR of carbonisation process. Figure 5 shows the TGA curve and weight percent derivative of palm frond degradation. It shows that the first weight loss occurred at 100°C with moisture loss.

The evolving moisture can also be detected in the FTIR 3D diagram (Fig. 6). There are two peaks of the O–H functional group, stretching at 3600–3000 cm^{-1} and bending at 1440–1400 cm^{-1}, that signify the presence of water. Moisture continues to evolve up till 150°C, when the weight loss halts (Fig. 5). The weight loss resumes at approximately 220°C, when CO_2 and water begin to leave the system again. The evolution of CO_2 is identified around the 2200–2400 cm^{-1} region

https://doi.org/10.1017/S1755691012000035 Published online by Cambridge University Press

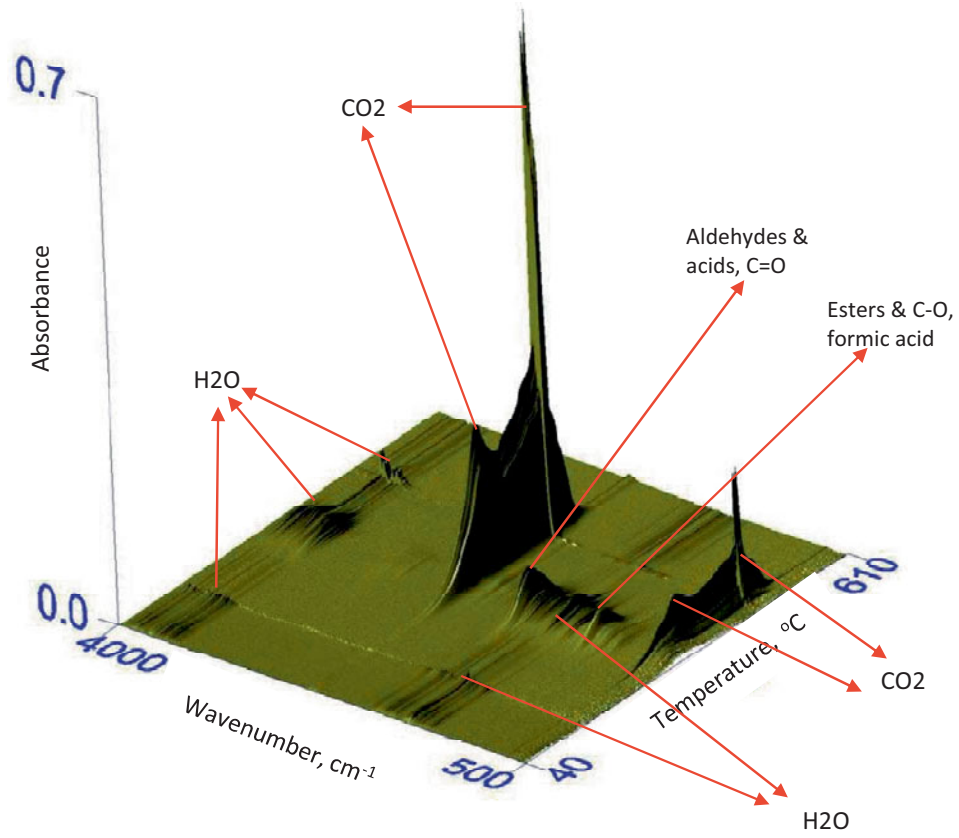


Figure 6 TGA-FTIR 3D diagram of gas evolution during carbonisation of palm frond.

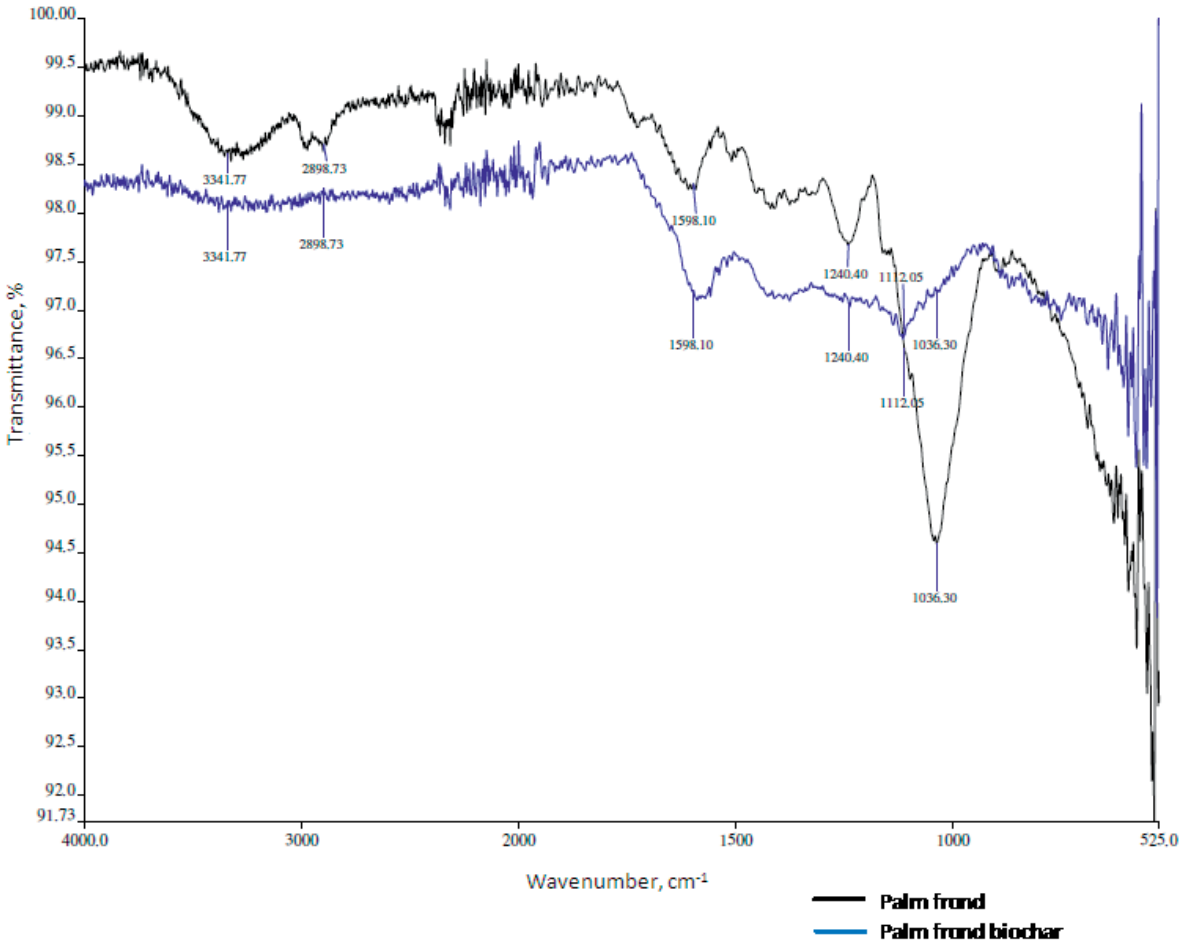


Figure 7 FTIR spectrum of palm frond and palm frond biochar.

https://doi.org/10.1017/S1755691012000035 Published online by Cambridge University Press

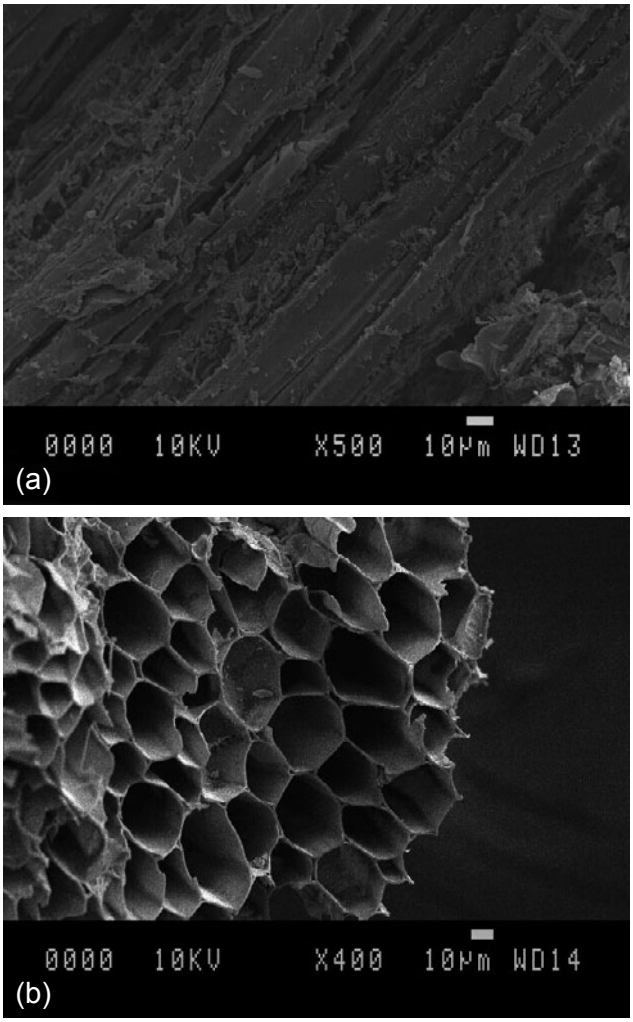


Figure 8 SEM images of palm frond: (a) before carbonisation; (b) after carbonisation.

(Fig. 6), due to the stretching of C=O, and at 666 cm^{-1}. Yang *et al.* (2006) found that hemicelluloses started to degrade in the 220–315°C temperature range and that depolymerisation of cellulose occurs between 250°C and 350°C. Significant mass loss was observed in the TGA curve. At 250°C, gases other than CO_2 also start to de-gas. These gases were detected in the FTIR at the wavelength 1792 cm^{-1} (aldehyde), and at 1170 cm^{-1} due to the stretching vibration of C–O–C in ethers or esters. These gases continued to evolve until the temperature reached 350°C. Three other significant mass loss peaks also occurred at 315°C, 350°C and 400°C. These are the periods where amorphous carbon matrix is created during thermal degradation of lignocellulosic biomass. The matrix later grows into a polyaromatic graphene sheet (Paris *et al.* 2005). Large releases of CO_2 and water in the FTIR spectrum at 450°C correspond to the final weight reduction to 5% of the palm frond's original weight. This weight remained unchanged until the final temperature of 610°C.

2.2. Characterisation of palm frond biochar

2.2.1. FTIR, SEM and BET. The FTIR spectra of palm frond before and after carbonisation were compared against those in the Infrared and Raman Characteristic Group Frequencies, Tables and Charts (Socrates 2004). IR spectra of palm frond before carbonisation show two distinctive peaks: one at 3341 cm^{-1} that is indicative of stretching of the O–H functional group; and one at 2898 cm^{-1} that is cause by the carbon backbone C–H stretching (Fig. 7).

The absorption bands at 1240 cm^{-1} were also observed, arising from the stretching vibration of the C–O group, and, together with symmetrical C–O–C stretching at 1036 cm^{-1} and 1242 cm^{-1}, confirm the presence of either esters or ethers. These peaks are eliminated after carbonisation. The existence of an aromatic skeleton vibration C–C bond at 1598 cm^{-1} is clearly visible in the palm frond and it remains intact after carbonisation. This signifies that the aromatic ring of lignin did not disintegrate during carbonisation of the biochar at a temperature of 320°C.

The palm frond biochar was prepared by heating it up to about 320°C. At this temperature, it still retained approximately 50% of its final weight. Based on Yang *et al.* (2006), the cross-point between hemicelluloses and cellulose degradation is at 315°C. At 320°C, most of the hemicelluloses would have fully disintegrated, but depolymerisation of cellulose would still be incomplete. Most of the lignin aromatic structure would still be available, and this can be seen from the still-intact aromatic vibration at 1598 cm^{-1} in the biochar's FTIR spectrum. Lignin is the main component in any char production (Yang *et al.* 2006).

The scanning electron microscope (SEM) images in Figure 8 show palm frond before and after carbonisation; the major components of palm frond would be cellulose, hemicelluloses and lignin (Khalil *et al.* 2012). SEM cross-section images of the biochar show the existence of macropores (>50 nm) that most probably originate from lignin. Lignin has been reported to fuse on pyrolysis and forms macropores of ~25 μm to ~100 μm in size (Raveendran *et al.* 1996).

Table 2 Surface properties of palm frond, palm frond biochar and the two lump wood biochars.

			Biochar			
		Palm Frond	Palm Frond	Lump Wood 1	Lump Wood 2	Activated carbon
Surface Properties		m^2/g	m^2/g	m^2/g	m^2/g	m^2/g
1	BET Surface Area	4	9	35	182	322
2	Langmuir Surface Area	8	18	46	241	436
3	BJH Adsorption cumulative surface area of pores	2·6	6·4	0·2	10·7	160·8
		cm^3/g	cm^3/g	cm^3/g	cm^3/g	cm^3/g
4	BJH Adsorption cumulative volume of pores	0·01	0·02	0·01	0·02	0·24
		nm	nm	nm	nm	nm
5	BJH Adsorption average pore diameter (4V/A):	17·1	10·6	107·7	6·1	6

https://doi.org/10.1017/S1755691012000035 Published online by Cambridge University Press

Table 3 pH and CEC value of palm frond biochar compares to the two lump wood biochar.

Biochar	pH Value	CEC (cmol/kg)
Palm frond	9·5	210
Lump wood 1	8·0	29
Lump wood 2	8·4	39

Table 4 pH and CEC value of several biochars.

Biochar feedstock	pH	CEC cmol/kg	Reference
Bark of *Acacia* tree	7·4	37	Yamato *et al.* 2006
Douglas fir (heated at 350°C)	4·2	21	Gundale & DeLuca 2006
Douglas fir (heated at 800°C)	9	19	
Ponderosa pine (heated at 350°C)	4·5	23	
Ponderosa pine (heated at 800°C)	9·2	17	
Green waste	9·4	24	Chan *et al.* 2007
Hardwood	–	23	Gaskin *et al.* 2009
Peanut hull	–	44	
Pine chip	–	27	
Poultry litter	9·9	–	Chan *et al.* 2008
Sewage sludge	8·1	35	Hossain *et al.* 2010

Biochar's porous structure consists of micropores (<2 nm), mesopores (2–50 nm) and macropores (>50 nm) (Wildman & Derbyshire 1991). The adsorption of small molecules such as gases and common solvents occur at the micropore level, but larger molecules such as colours and probably other organics are adsorbed in mesopores. The BET (Brunauer–Emmett–Teller) surface area and BJH (Barret–Joyner–Halenda) pore volume and width are reported for the palm frond biochar in Table 2. The BET surface area of the palm frond was originally 4 m^2/g, and it increased to 8 m^2/g upon carbonisation, which is low compared to lump wood charcoal and activated carbon. The average pore diameter measured by BJH adsorption is 10 nm (mesopores).

2.2.2. pH and CEC. Palm frond biochar has a high pH of 9·5 and a CEC value of 210 cmol/kg (Table 3). The pH and cation exchange capacity of biochar from several sources has been reported by many (Table 4). However, due to differences in the methods of testing, it may not be practical to compare results. Palm frond biochar releases very high concentrations of cations as compared to the other two biochars (Fig. 9), especially K^+ ions.

The ratio of K^+ released is relatively high as compared to Mg^{2+}, Na^+ or Ca^{2+} ions (Fig. 10a). This ratio is slightly different for lump wood 1, where Ca^{2+} is the major cation released (Fig. 10b), and lump wood 2, where the ratio between Ca^{2+} and K^+ is about the same as that of the major cations (Fig. 10c). The high K^+ ions released from the palm frond biochar may have been due to its original materials. Potassium fertiliser is used extensively in the cultivation of oil palm trees, and the ions might have accumulated in the fronds.

2.3. Sorption capacity of palm frond biochar

Adsorption isotherm studies were conducted to estimate the maximum adsorption capacity of palm frond biochar for four heavy metals (Pb^{2+}, Cu^{2+}, Ni^{2+} and Zn^{2+}) at 25°C as compared to two lump wood charcoals; activated carbon was used as a reference adsorbent. The Langmuir (Langmuir 1918) and Freundlich (Freundlich & Helle 1939) models were used to fit the experimental data. Table 5 shows that the experimental data fit the Langmuir model better than they do the Freundlich model, with correlation coefficients of palm frond biochar adsorption for all metals being ≥0·92. The model predicts the following adsorption rates: Pb^{2+} 83·3 mg/g; Cu^{2+} 41·4 mg/g; Ni^{2+} 13·0 mg/g; and Zn^{2+} 19·7 mg/g. These predictions correlate well with the following experimental data on adsorption rates: Pb^{2+} 83·7 mg/g; Cu^{2+} 47·5 mg/g; Ni^{2+} 13·1 mg/g; and Zn^{2+} 19·7 mg/g. The palm frond biochar has affinities with metal ions in the following order: $Pb^{2+} > Cu^{2+} > Zn^{2+} > Ni^{2+}$, which is a similar order to those reported for lignin (Guo *et al.* 2008). The biochar was produced

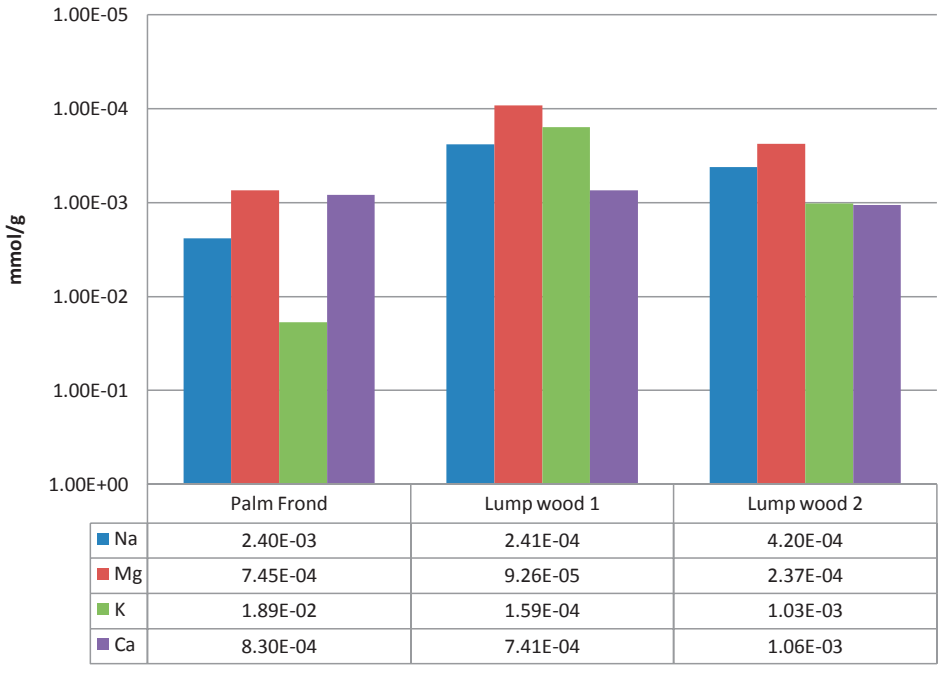


Figure 9 Comparison of the type of cations released by each biochar after one hour agitation.

https://doi.org/10.1017/S1755691012000035 Published online by Cambridge University Press

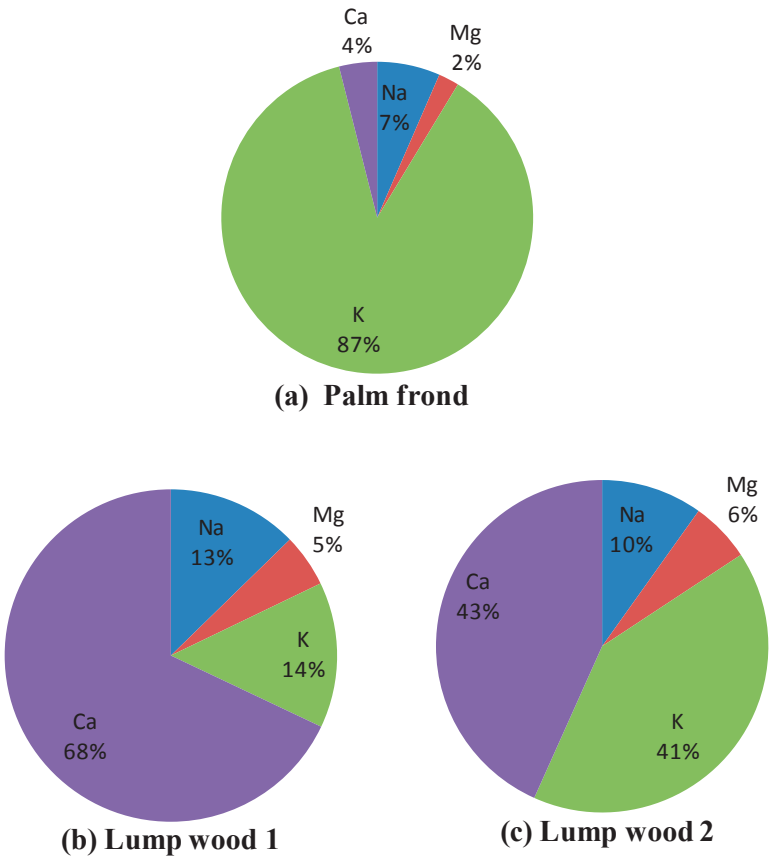


Figure 10 Percentage of cations produced from (a) palm frond (b) lump wood charcoal 1 (c) lump wood charcoal 2.

Table 5 Summary of adsorptions capacity with correspondent correlation coefficient R^2 of the fitted linear curve.

Biochar	Pb^{2+}				Cu^{2+}				Nl^{2+}				Zn^{2+}			
	Langmuir		Freundlich		Langmuir		Freundlich		Langmuir		Freundlich		Langmuir		Freundlich	
	Q°	R^2	Kr	R^2	Q°	R^2	Kr	R^2	Q°	R^2	Kr	R^2	Q°	R^2	Kr	R^2
Lumpwood 1	7·74	0·9973	3·11	0·3992	2·19	0·9770	0·19	0·8369	0·51	0·8312	0·04	0·9471	1·28	0·8611	0·32	0·0509
Lumpwood 2	37·17	0·9971	6·72	0·2633	10·10	0·9622	0·70	0·7694	1·83	0·9888	0·28	0·7939	8·20	0·9888	0·60	0·8434
Palm frond	83·30	0·9998	12·27	0·5668	41·39	0·9456	6·52	0·9557	12·99	0·9995	1·70	0·8633	19·74	0·9998	6·11	0·8936
Activated carbon	282·21	0·9322	7·44	0·8455	31·85	0·6397	2·60	0·5327	12·47	0·9723	1·21	0·8668	14·87	0·9805	2·04	0·9022

at the maximum temperature of 320°C and, based on cellulose, hemicelluloses and lignin pyrolysis curves, approximately 80–90% of the original cellulose and lignin would still be available in the biochar (Yang *et al.* 2006). The existence of aromatic vibration at 1598 cm^{-1} in the biochar's FTIR spectrum, similar to that of the original palm frond, signifies the availability of a lignin aromatic benzene ring. Table 6 compares the adsorption capacity of palm frond biochar with other reported findings. The adsorption rates of Pb^{2+} by the two lump wood biochars were comparable to those cited in the literature for biochars made from woody material (Machida *et al.* 2006; Mohan *et al.* 2007; Liu & Zhang 2009).

3. Discussion

The results of this study show that the heat and soots from the burning of palm frond in the earth pit change the pH value and organic content of the earth wall, resulting in a more fertile soil compared to the existing one. The effect on the soil texture is not noticeable, which may reflect the short duration of the fire. Replication of the carbonisation process in the TGA–FTIR indicates that the materials remaining in the biochar are mainly lignin and some cellulose, as is confirmed by the FTIR spectrum of the biochar. The FTIR spectrum from TGA–FTIR analysis also identifies the type of gases released in the smoke during charring of the palm frond as carbon monoxide, esters, aldehyde and ethers. The carbonisation process normally produces substances that can be harmful and pollute the environment (FAO 1983), and simple precautions, such as locating the charring area away from residential areas, will minimise exposure. The pH, CEC and type of cations released indicate whether the biochar would be beneficial as a soil ameliorant. SEM and BET analyses of the structural properties of palm frond biochar indicate the pore types available, which is important for the study of heavy metal adsorptions. Heavy metal adsorption of palm frond biochar showed similarity to the adsorption of heavy metals by lignin.

https://doi.org/10.1017/S1755691012000035 Published online by Cambridge University Press

Table 6 Approximate adsorption capacity of palm frond biochar for heavy metals compares to those of other feedstock.

Biochar feedstock	Metal	Approximate Adsorption Capacity mg/g	Reference
Rice husk	Pb^{2+}	2	Liu & Zhang 2009
Oak wood	Pb^{2+}	3	Mohan *et al.* 2007
Pine bark	Pb^{2+}	3	Mohan *et al.* 2007
Pine wood	Pb^{2+}	4	Mohan *et al.* 2007
Pine wood	Pb^{2+}	4	Liu & Zhang 2009
Bamboo	Pb^{2+}	11	Lalhruaitluanga *et al.* 2010
Oak bark	Pb^{2+}	13	Mohan *et al.* 2007
Palm frond	Pb^{2+}	83	–
Dairy manure	Pb^{2+}	141	Cao *et al.* 2009
Oak wood	Pb^{2+}	143	Machida *et al.* 2006
Peanut husk	Pb^{2+}	180	Ricordel 2001
Pogamia pinnata pods	Pb^{2+}	370	Nadeem *et al.* 2009
Rice husk	Cu^{2+}	2	Ong *et al.* 2007
Bone	Cu^{2+}	27	Wilson *et al.* 2003
Palm frond	Cu^{2+}	41	–
Nettle	Cu^{2+}	300	Wingate 2008
Peanut husk	Ni^{2+}	16	Ricordel 2001
Palm frond	Ni^{2+}	13	–
Peanut husk	Zn^{2+}	13	Ricordel 2001
Palm frond	Zn^{2+}	20	–
Bone	Zn^{2+}	24	Wilson *et al.* 2003

4. Conclusions

Palm frond biochar has great potential to adsorb heavy-metal contaminants with minimum production costs. It has a porous structure, with large numbers of mesopores that may also be beneficial in adsorbing organic pollution. It has high pH and CEC values that can be used to ameliorate acidic tropical soil. High soluble K^+ in the biochar may also prove effective as a source of slow-release fertilisers in tropical countries that receive high rainfalls.

5. References

Babel, S. & Kurniawan, T. A. 2003. Low-cost adsorbents for heavy metals uptake from contaminated water: a review. *Journal of Hazardous Materials* **B97**, 219–43.

Bailey, S. E., Olin, T. J., Bricka, M. & Adrian, D. D. 1999. A Review of potentially low-cost sorbents for heavy metals. *Water Research* **33**, 2469–79.

Beesley, L. & Marmiroli, M. 2011. The immobilisation and retention of soluble arsenic, cadmium. *Environmental Pollution* **159**, 474–80.

Cao, X., Ma, L., Gao, B. & Harris, W. 2009. Dairy-Manure Derived Biochar Effectively Sorbs Lead and Atrazine. *Environmental Science and Technolology* **43**, 3285–91.

Chan, K. Y., Van Zwieten, L., Meszaros, I., Downie, A. & Joseph, S. 2007. Agronomic values of green waste bio-char as a soil amendment. *Australian Journal of Soil Research* **45**, 629–34.

Chan, K. Y., Van Zwieten, E. L., Meszaros, I., Downie, A. & Joseph, S. 2008. Using poultry litter biochars as soil amendments. *Australian Journal of Soil Research* **46**, 437–44.

Chen, S., Zhu, Y., Ma, Y. & McKay, G. 2006. Effect of bone char application on Pb bioavailability. *Environmental Pollution* **139**, 433–39.

Chidumayo, E. N. 1994. Effects of wood carbonization on soil and initial development of seedlings in miombo woodland, Zambia. *Forest Ecology and Management* **70**, 353–57.

Derenne, S. & Largeau, C. 2001. A review of some important families of refractory macromolecules: Composition, origin and fate in soil and sediments. *Soil Science* **166**, 833–47.

FAO. 1983. *Chapter 4: Carbonisation processes.* Retrieved September 27, 2012, from FAO Corporate Document Repository: http://www.fao.org/docrep/X5328e/x5328e05.htm#chapter 4 carbonisation processes.

Freundlich, H., & Helle, W. 1939. The Adsorption of cis- and trans-Azobenzene. *Journal of the American Chemical Society* **61**, 2228–30.

Gaskin, J. W., Das, K. C., Tassistro, A. S., Sonon, L. & Harris, K. 2009. Characterization of Char for Agricultural Use in the Soils of the Southeastern United States. *In* Woods, W. I., Teixeira, W. G., Lehmann, J., Steiner, C., WinklerPrins, A. M. G. A. & Rebellato, L. (eds) *Amazonian Dark Earths: Wim Sombroek's Vision,* 433–43. Netherlands & New York: Springer Science + Business Media B.V.

Gillman, G. P. & Sumpter, E. A. 1986. Modification to the compulsive exchange method for measuring exchange characteristics of soils. *Australian Journal of Soil Research* **24**, 61–66.

Glaser, B., Lehmann, J. & Zech, W. 2002. Ameliorating physical and chemical properties of highly weathered soils in the tropics with charcoal – a review. *Biology and Fertility of Soils* **35**, 219–30.

Gundale, M. J. & DeLuca, T. H. 2006. Temperature and substrate influence the chemical properties of charcoal in the ponderosa pine/Douglas-fir ecosystem. *Forest Ecology and Management* **231**, 86–93.

Gupta, V. K., Carrot, P. J. M., Ribeiro-Carrot, M. M. L. & Suhas. 2009. Low-cost adsorbents: growing approach to wastewater treatment – a review. *Critical Reviews in Environmental Science and Technology* **39**, 783–842.

Guo, X., Zhang, S. & Shan, X. 2008. Adsorption of metal ions on lignin. *Journal of Hazardous Materials* **151**, 134–42.

Hossain, M. K., Strezov, V., Chan, K. Y. & Nelson, P. F. 2010. Agronomic properties of wastewater sludge biochar and bioavailability of metals in production of cherry tomato (*Lycopersicon esculentum*). *Chemosphere* **78**, 1167–71.

Ketterings, Q. M., Bigham, J. M. & Laperche, V. 2000. Changes in soil mineralogy and texture caused by slash-and-burn fires in Sumatra, Indonesia. *Soil Science Society of America Journal* **64**, 1108–17.

Khalil, A., Jawaid, M., Hassan, A., Paridah, M. T. & Zaidon, A. 2012. Oil palm biomass fibres and recent advancement in oil palm biomass fibres based hybrid biocomposites. *In* Hu, N. (ed.) *Composites and Their Applications*, 187–220. InTech.

Lalhruaitluanga, H., Jayaram, K., Prasad, M. N., & Kumar, K. K. 2010. Lead(II) adsorption from aqueous solutions by raw and activated charcoals of *Melocanna baccifera* Roxburgh (bamboo) – a comparative study. *Journal of Hazardous Materials* **175**, 311–18.

Langmuir, I. 1918. The adsorption of gases on plane surfaces of glass, mica and platinum. *Journal of the American Chemical Society* **40**, 1361–403.

Lehmann, J., da Silva Jr., J. P., Steiner, C., Nehls, T., Zech, W. & Glaser, B. 2003. Nutrient availability and leaching in an archeological anthrosol and a ferrasol of the Central Amazon basin: fertilizer, manure and charcoal ammendments. *Plant and Soil* **249**, 343–57.

Lehmann, J. L. Gaunt, J. & Rondon, M. 2006. Bio-char Sequestration in Terrestrial Ecosystem – A Review. *Mitigation and Adaptation Strategies for Global Change* **11**, 403–27.

Lehmann, J. L. & Joseph, S. 2009. Biochar for Environmental Management: An Introduction. *In* Lehmann J. L. & Joseph, S. (eds) *Biochar Environmental Management Science and Technology*, 1–12. London: Earthscan.

Lewis, I. C. 1982. Chemistry of Carbonization. *Carbon* **20**(6), 519–29.

Liu, Z. & Zhang, F. 2009. Removal of lead from water using biochars prepared from hydrothermal liquefaction of biomass. *Journal of Hazardous Materials* **167**, 933–39.

Machida, M., Yamazaki, R., Aikawa, M., & Tatsumoto, H. 2006. Role of minerals in carbonaceous adsorbents for removal of Pb(II) ions from aqueous solution. *Separation and Purification Technology* **46**, 88–94.

Mohan, D., Pittman, C., Brick, M., Smith, F. and Yancey, B. 2007. Sorption of arsenic, cadmium, and lead by chars produced from fast pyrolysis of wood and bark during bio-oil production. *Journal of Colloid and Interface Science* **310**, 57–73.

Nadeem, R., Ansari, T. M., & Akhtar, A. M. 2009. Pb(II) Sorption by Pyrolysed *Pongamia pinnata* Pods Carbon (PPPC). *Chemical Engineering Journal* **152**, 54–63.

Oguntunde, P. G., Fosu, M., Ajayi, A. E. & van de Giesen, N. 2004. Effects of charcoal production on maize yield, chemical properties and texture of soil. *Biology and Fertility of Soils* **39**, 295–99.

Ong, S., Seng, C. & Lim, P. 2007. Kinetics Of Adsorption Of Cu(Ii) And Cd(Ii) From Aqueous Solution On Rice Husk And Modified Rice Husk. *Electronic Journal of Environmental, Agricultural and Food Chemistry* **6**, 1764–74.

Paris, O., Zollfrank, C. & Zickler, G. 2005. Decomposition and carbonisation of wood biopolymers – a microstructural study of softwood pyrolysis. *Carbon* **43**, 53–66.

https://doi.org/10.1017/S1755691012000035 Published online by Cambridge University Press

Raveendran, K., Ganesh, A. & Khilar, K. 1996. Pyrolysis characteristics of biomass and biomass components. *Fuel* **75**, 987–98.

Ricordel, S., Taha, S., Cisse, I. & Dorange, G. 2001. Heavy metals removal by adsorption onto peanut husks carbon: characterization, kinetic study and modeling. *Separation and Purification Technology* **24**, 389–401.

Socrates, G. 2004. *Infrared and Raman Characteristic Group Frequencies.* Chichester, UK: John Wiley & Sons Ltd.

Steiner, C., Teixeira, W. G., Lehmann, J., Nehls, T., deMacedo, J. L. V., Blum, W. E. & Zech, W. 2007. Long term effects of manure, charcoal and mineral fertilization on crop production and fertility on a highly weathered Central Amazonian upland soil. *Plant and Soil* **291**, 275–90.

Steiner, C., Teixeira, W. G., Woods, W. I. & Zech, W. 2009. Indigenous Knowledge About *Terra Preta* Formation. *In* Woods, W. I., Teixeira, W. G., Lehmann, J., Steiner, C., WinklerPrins, A. M. G. A. & Rebellato, L. (eds) *Amazonian Dark Earths: Wim Sombroek's Vision*, 193–204. Netherlands & New York: Springer Science + Business Media BV.

Steward, F. R., Peter, S. & Richon, J. B. 1990. A method for predicting the depth of lethal heat penetration into mineral soils exposed to fires of various intensities. *Canadian Journal of Forest Research* **20**, 919–26.

Tryon, E. 1948. Effect of charcoal on certain physical, chemical and biological properties of forest soils. *Ecological Monograph* **18**, 81–115. Washington, DC: Ecological Society of America.

Uchimiya, M., Klasson, K., Wartelle, L. & Lima, I. 2011. Influence of soil properties on heavy metal sequestration by biochar amendment. *Chemosphere* **82**, 1431–37.

Wildman, J. & Derbyshire, F. 1991. Origins and functions of macroporosity in activated carbons from coal and wood precursors. *Fuel* **70**, 655–61.

Wilson, J. A., Pulford, I. D. & Thomas, S. 2003. Sorption of Cu and Zn by bone charcoal. *Environmental Geochemistry and Health* **25**, 51–56.

Wingate, J. R. 2008. *Development Of Novel Charcoals For The Sorption And Transformation Of Heavy Metals In Contaminated Land.* PhD Thesis, University of Surrey, UK.

Yaman, S. 2004. Pyrolysis of biomass to produce fuels and chemical feedstocks. *Energy Conversion and Management* **45**, 651–71.

Yamato, M., Oimori, Y., Wibowo, I. F., Anshori, S. & Ogawa, M. 2006. Effects of the application of charred bark of *Acacia mangium* on the yield of maize, cowpea and peanut, and soil chemical properties in South Sumatra, Indonesia. *Soil Science and Plant Nutrition* **52**, 489–95.

Yang, H., Yan, R., Chen, H., Zheng, C., Lee, D. & Liang, D. 2006. In-Depth Investigation of Biomass Pyrolysis Based on Three Major Components: Hemicellulose, Cellulose and Lignin. *Energy & Fuels* **20**, 388–93.

MS received 26 October 2011. Accepted for publication 15 November 2012.

https://doi.org/10.1017/S1755691012000035 Published online by Cambridge University Press